Chapter 9
Understanding Fabrication and Properties of Magnesium Matrix Nanocomposites

Sudip Banerjee, Suswagata Poria, Goutam Sutradhar, and Prasanta Sahoo

1 Introduction

Composites are well-known high-class materials which possess superiority than monolithic counterparts having unique capability of improving typical qualities of monolithic alloys [78, 79]. Enhancement of such properties of monolithic alloy can be restrained by perfectly selecting principle elements of composite design (size, type and amount). Primarily, research on metal matrix composites (MMCs) got momentum in 1970s. At that time, researchers mainly used powder metallurgy, stir casting and rheo-casting processes to develop MMCs by incorporating ceramic reinforcements and achieved impressive results [20, 45]. Improvements of typical properties, like elastic modulus, damping capability, creep behavior and wear resistance, were proclaimed [25, 39]. Researchers have incorporated micron scale continuous and discontinuous reinforcements in different metal matrix prior to twentieth century. But some limitations, like high cost, application in highly specialized area (space sector) and complex synthesis process, were observed for continuously reinforced MMCs. Conversely, MMCs with discontinuous reinforcement were successfully fabricated through different fabrication techniques [26, 68]. Around 2000, interest on nanoparticles was generated as reinforcement in metal matrix due to advancement in nano-science. In this regard, Al, Mg, Ni, Ti and Cu were mainly considered [26, 69]. In this study, concentration is given on magnesium as base metal because pure magnesium and magnesium alloys are extremely lightweight than other majorly used

S. Banerjee (✉) · P. Sahoo
Jadavpur University, Kolkata, India
e-mail: banerjee.sudip71@gmail.com

S. Poria
Heritage Institute of Technology, Kolkata, India

G. Sutradhar
National Institute of Technology, Manipur, India

S. Sahoo (ed.), *Recent Advances in Layered Materials and Structures*,
Materials Horizons: From Nature to Nanomaterials,
https://doi.org/10.1007/978-981-33-4550-8_9

metals, i.e., 77% lighter than steel, 33% lighter than aluminum and 61% lighter than titanium. Being the lightest metal, magnesium alloys also have good machinability (>50% Al), good damping capability and superb castability (>25–50% Al).

Nowadays, ceramic-based and carbon-based particles are procurable at much lower price than 1980–90s which promotes impressive increase in research and development of Mg-MMNCs. Moreover, incorporation of nanoscale reinforcement produces promising results by enhancing a number of typical properties. Normally, reinforcement particles are selected from carbide, nitride, oxide, boride and carbon families, especially Al_2O_3, SiC, B_4C, BN, TiB_2, AlN, CNT and graphite, to incorporate in metal matrix [73]. Through this incorporation, some typical properties, i.e., ductility, compressive and tensile property, creep, damping, elevated temperature mechanical properties, coefficient of thermal expansion (CTE), machining, wear resistance, friction behavior, corrosion resistance, ignition resistance, etc., were noticeably enhanced.

However, properties of MMNCs also depend on some other factors, i.e., primary and secondary fabrication process, process parameters, size of reinforcement, matrix metal, etc. In regard to fabrication of Mg metal matrix nanocomposites (Mg-MMNCs), agglomeration of nanoparticles, low wettability between nanoparticles and base matrix are of main concern. Fabrication methods of Mg-MMNCs are quite similar to Mg-MMCs. These processes are either solid processing or liquid metallurgy route. In liquid metallurgical method, stir casting, disintegrated melt deposition (DMD) and ultrasonic stirring technique (UST) are mostly used processing method. In stir casting, an impeller is employed in molten metal. Hence, stirring parameters, i.e., stirrer speed, stirrer location and stirrer design are significant parameters [1, 2]. In UST, high-frequency ultrasonic cavitation is applied to disperse nanoparticles which employ micro-hot spots, acoustic streaming and very high temperature to break agglomeration and disperse particles [53]. DMD is a spray-type processing method, in which molten composite is disintegrated prior to deposition [32]. Besides, some secondary processing like rolling, extrusion may be employed to further improve properties (refining grains, crushing secondary phase) or providing necessary shapes of composites.

In view of possible application of magnesium nanocomposites, the present study attempts to present a thorough review emerged on works and multi-dimensional sagacity of scientific community. Key points which are considered are as follows: (1) present status of fabrication method of Mg-MMNCs following liquid metallurgy, (2) strengthening mechanism of Mg-MMNCs, (3) mechanical properties of Mg-MMNCs, (4) tribological properties of Mg-MMNCs and (5) corrosion behavior of Mg-MMNCs.

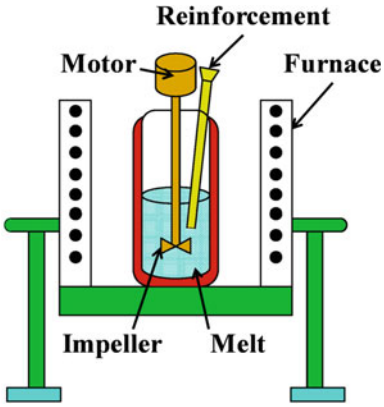

Fig. 1 Schematic diagram of stir casting

2 Preparation of Magnesium Matrix Composite Reinforced by Nanoparticles

2.1 Stir Casting

Stir casting is very naive and economical technique in which particles are incorporated in liquid metal using mechanical stirrer. Schematic diagram of stir casting process is presented in Fig. 1. Existing literature discloses that stir casting is extensively adopted to incorporate metal oxides, nitrides, carbide microparticles in magnesium matrix but limited numbers of literatures are available on incorporation of nanoparticles in magnesium matrix through this process. Main constraints of stir casting process are below par wettability of nanoparticles in molten metal, air entrapment due to rotation of stirrer and clusters of nanoparticles [3, 10, 11]. However, Habibnejad-Korayem et al. [35] have attempted to incorporate Al_2O_3 nanoparticles in Mg-matrix through stir casting method and reported homogeneous distribution of particles in magnesium matrix. Karuppusamy et al. [42] have incorporated WC nanoparticles in AZ91 melt using vacuum-assisted stir casting and achieved homogeneous distribution.

2.2 Ultrasonic Vibration

2.2.1 Principle of Ultrasonic Cavitation and Acoustic Streaming

Normally, high surface area of nanoparticles results in agglomeration in molten magnesium. Furthermore, wettability between Mg-melt and surfaces of nanoparticles is poor. In this regard, ultrasonic treatment (UST) is a widely used method to

effectively disburse nanoparticles in magnesium melt. Schematic diagram of ultrasonic vibration is shown in Fig. 2. Application of UST in Mg-melt generates different effects like cavitation and acoustic streaming. At the time of UST, application of high-frequency ultrasound through sonotrode generates alternating expansion and compression in definite area of melt near sonotrode. During expansion, small cavities in the form of cavitation bubble form for short duration [68]. These bubbles collapse and generate high pressure (1000 atm) as well as high temperature (several thousand degrees). On the other hand, agglomerated particles also include some entrapped gas. These gas bubbles also collapse and exert high intensity force which may exceed the Van der Waals force of agglomerated particles. At that instant, the agglomerated clusters are shattered which results in small clusters or individual particles. With repetition of this cavity formation and destruction, millions of shock waves generate in melt and disintegrate the agglomerated nanoparticles. Schematic diagram of de-agglomeration of nanoparticles due to acoustic streaming is shown in Fig. 3, and schematic diagram of effect of entrapped gas as well as sonotrode is shown in Fig. 4.

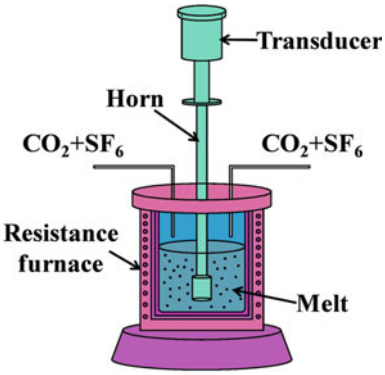

Fig. 2 Schematic diagram of ultrasonic vibration

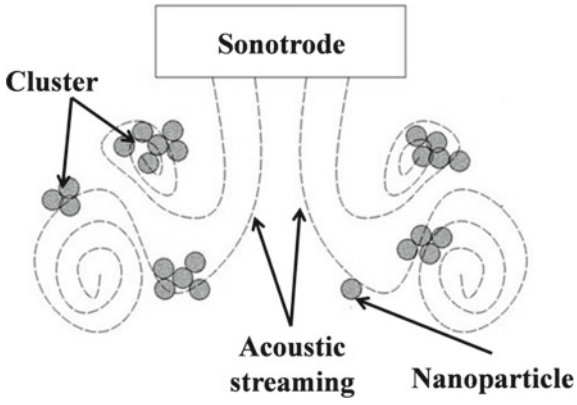

Fig. 3 Schematic diagram of de-agglomeration of nanoparticles due to acoustic streaming

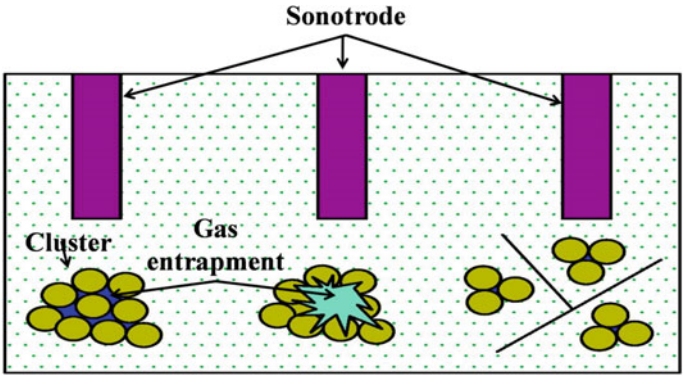

Fig. 4 Schematic diagram of effect of entrapped gas as well as sonotrode

Furthermore, UST causes acoustic streaming which depends on viscosity of melt, melt temperature and ultrasonic intensity. Eskin et al. [26] have described three types of acoustic streaming: (1) Schlichting flow which occurs at phase interfaces. These interfaces involve cavitation bubble. Heat and mass transfer is considered in this flow, (2) acoustic streaming of standing wave field and (3) acoustic streaming of bulk metal melt which develops by absorbing momentum of ultrasound flow. Hence, cavitation and acoustic streaming both help to disperse particles and contribute in grain refinement. In this context, Ishiwata et al. [40] have developed model on acoustic streaming separately for water and Al-melt. It is reported that acoustic streaming is mainly controlled by amplitude of ultrasonic vibration.

2.2.2 Effect of Ultrasound on Magnesium Alloy

Ramirez et al. [64] have discussed ultrasonic intensity (I) as follows:

$$I = \frac{\rho c (2\pi f A)^2}{2} \tag{1}$$

where ρ = density of molten metal, c = ultrasonic velocity, f = ultrasonic frequency and A = amplitude of horn. Eskin et al. [26] have reported that if intensity value exceeds 80 W cm^{-2} then generated cavitations are adequate for magnesium melt. Hence, ultrasonic intensity and corresponding wavelength can be regulated by following Eq. (1) to indulge specific requirement at the time of fabricating Mg-MMNC. Chen et al. [13] have shown the effect of ultrasonic vibration on capillary effect by improving penetration of melt in agglomerated nanoparticle. Critical osmotic pressure (p_s) is expressed by

$$p_s = \frac{6\lambda\sigma_{LG}\mathrm{Cos}\Theta(\emptyset - 1)}{d_{p\times}\emptyset} \tag{2}$$

where λ = geometric factor, d_p = average particle diameter, Θ = contact angle of particle and melt, σ_{LG} = surface tension and $\emptyset$ = volume fraction of particle porosity. Using Eq. (2), Nie et al. [58, 59] have found p_s to achieve required wettability of SiC nanoparticles in Mg-melt.

Accordingly, researchers have used UST to disperse nanoparticles in molten magnesium. Cao et al. [10] have incorporated AlN nanoparticles in AZ91 alloy using UST and achieved homogeneous distribution. Katsarou et al. [43] have incorporated AlN nanoparticles (1 wt%) in Elektron21 alloy using UST (0.3 kW and 20 kHz) and achieved refined grain along with enhanced mechanical properties. Khandelwal et al. [44] have employed UST to fortify nano-sized Al_2O_3 (0.5, 1 and 2 wt%) in AZ31 alloy in two conditions, i.e., during air cooling and isothermal in furnace. Lan et al. [48], Erman et al. [23] and Nie et al. [58, 59] have fortified SiC nanoparticles with different weight percentage in magnesium alloy with the help of high-frequency UST. Lan et al. [48] have incorporated 2 and 5 wt% SiC by applying 80 W ultrasonic power and reported fair distribution of SiC particles. Cao et al. [11] have reinforced 2 wt% SiC particles in molten Mg by inserting (25–31 mm) niobium probe into melt and applying 4.0 KW power and 17.5 kHz frequency. Erman et al. [23] have reinforced 2 wt% nano-SiC in Mg through UST and reported 60% reduction in average grain size. Cicco et al. [18] have ultrasonically dispersed nano-sized SiC particles in Mg–Zn alloys and concluded that nanoparticle induction has better effect than direct strengthening for metallic metals. Habibnejad et al. [35] have developed Mg-Al_2O_3 nanocomposite by incorporating different weight percentage of Al_2O_3 nanoparticles in magnesium matrix using UST. Chen et al. [14] have applied combination of evaporation and UST to dense uniform dispersion of nano-sized reinforcement (14 vol% SiC) in Mg-melt. Shiying et al. [67] have developed AZ91-SiC nanocomposites by incorporating different weight percentage (0.5, 1, 1.5 and 2%) of SiC particles (40 nm). Choi et al. [17] have fortified TiB_2 nanoparticles (25 nm) in AZ91D melt using niobium sonotrode which produce 20 kHz frequency and 60 μm amplitude. Bhingole and Chaudhari [9] have inoculated carbon black nanoparticles (42 nm) in different magnesium alloys using 20 kHz UST.

2.3 *Combination of Ultrasonic Vibration and Semisolid Stirring*

Further modification of UST is carried out in which both stirring of semisolid and application of UST in melt are combined. In this process, mechanical stirring normally helps in incorporating nanoparticles and UST helps to deal with agglomeration and wettability. Schematic diagram of combination of ultrasonic treatment and semisolid stirring is presented in Fig. 5. Following this process, Nie et al. [60] have used this technique to synthesize AZ91/SiC_p nanocomposite. Initially, preheated SiC nanoparticles (1 vol%, 60 nm) are initially brought in contact with semisolid matrix (550 °C) and mechanical stirring is conducted for 5–25 min. Then, UST is

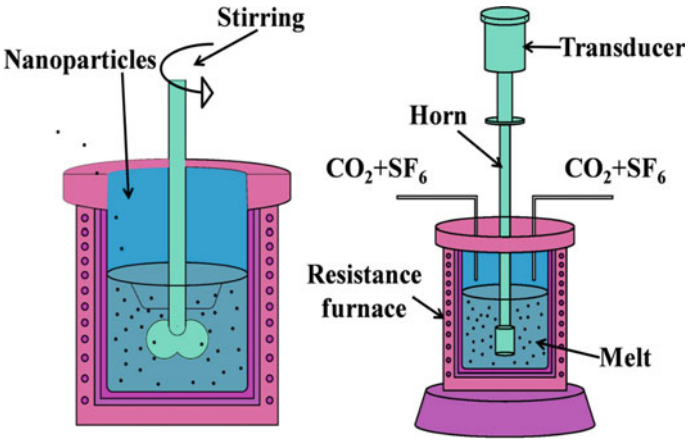

Fig. 5 Schematic diagram of combination of ultrasonic vibration and semisolid stirring

provided for 20 min at liquid state (700 °C) and solidified afterwards. Similarly, Shen et al. [66] have incorporated 3 vol% SiC nanoparticles in AZ31B matrix and observed no significant cluster of nano-SiC. Banerjee et al. [5–7] have incorporated WC nanoparticles (0.5, 1, 1.5 and 2 wt%) in AZ31 alloy using mechanical stirring as well as 20 kHz ultrasonic frequency and reported homogeneous distribution of nanoparticles in magnesium melt. Chen et al. [15] have used the same process (1400 rpm stirring, 20 kHz frequency and 60 μm amplitude) to incorporate high vol% SiC in Mg–Zn alloy. Liu et al. [52] have used the combination of mechanical stirring (300/500 rpm, 2 min) and ultrasonic vibration (20 kHz, 15 min) through titanium waveguide to incorporate CNT nanoparticles (20–40 nm). Zhou et al. [76] have produced Mg-hybrid composites by incorporating carbon nanotube and nano-SiC of different hybrid ratio through combination of mechanical stirring and ultrasonic vibration. Choi et al. [16] have employed the same process to develop Mg-1SiC nanocomposite using 3.5 kW power output and 17.5 kHz frequency for 15 min. In this process, a selective zone of melt pool is covered with 254 μm thin-walled truncated cone of niobium to confine SiC nanoparticles in that region.

2.4 Disintegrated Melt Deposition (DMD)

DMD technique possesses convenience of gravity die casting as well as spray forming, and in this process melting and pouring occur together. Schematic diagram of DMD process is presented in Fig. 6. In this process, atomized melt is rapidly solidified and low porosity, uniform grains as well as homogeneous distribution are found. But main limitation of this process is high viscosity of liquid melt with high volume percentage of reinforcement. Nguyen and Gupta [56] have tried DMD process to fortify Al_2O_3 in Mg-matrix and found equiaxed grain as well as good interfacial

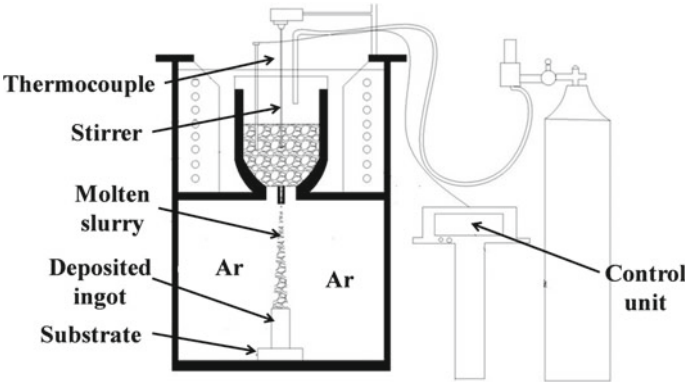

Fig. 6 Schematic diagram of DMD process

bonding. Hassan and Gupta [38] have attempted to use 1.1 vol% nano-Al_2O_3 (50 nm) following DMD process. Microstructural characterization revealed limited agglomeration and excellent distribution of particles throughout matrix. Goh et al. [32] have tried to incorporate CNT (0.3, 1.3, 1.6, 2 wt%) in magnesium through DMD process and observed microstructure as well as mechanical properties. Hassan and Gupta [36, 37] have incorporated nano-Y_2O_3/nano-ZrO_2 with varying weight percentages (0.22, 0.66 and 1.11 vol%) in Mg-matrix and reported good matrix-reinforcement interfacial integrity.

3 Secondary Processing Methods

Primary processed nanocomposites may have some defects or some microstructural irregularities which must be minimized or eliminated to improve typical properties. Hence, secondary processing techniques of nanocomposites are very essential. In secondary processing, either bulk material is deformed (extrusion, rolling, multidirectional forging) or severe plastic deformation is occurred (equal channel angular pressing, cyclic extrusion and compression).

3.1 Extrusion

In this secondary processing method, nanocomposite billets are pressurized in a die with high-pressure ram to minimize inappropriateness like voids, pores, cracks and cavity which are formed during primary processing. Schematic diagram of extrusion is shown in Fig. 7. This secondary processing method is typically applied at or above recrystallization temperature. In this process, main effective parameters are

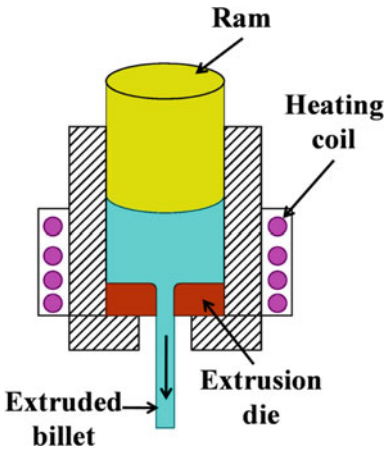

Fig. 7 Schematic diagram of extrusion

temperature, RAM speed and extrusion ratio, which should have optimum value to control oxidation and other noise factors. Nie et al. [60] have conducted hot extrusion on AZ91-SiC nanocomposites to further refine grain boundaries and reported that hot extrusion has further improved microstructural and mechanical properties than as-cast nanocomposites. Choi et al. [17] and Li et al. [49] have found similar results by applying hot extrusion. Occurrences of alignment of SiC particles toward direction of extrusion and grain refinement are documented.

3.2 Rolling

In rolling, high-pressure rolls are traveled over nanocomposites at plastic deformation stage to deform as-cast billets. High-pressure roll produces squeezing and compressive action which helps in further grain refinement. As a result, defects are eradicated and several typical properties are enhanced. In this process, key factors are number of passes and temperature. Wang et al. [72] have applied this process on AZ31/SiC nanocomposites and observed several beneficial effects on refined grains.

3.3 Multidirectional Forging (MDF)

In this process, the combination of plastic deformation and conventional mechanical process is applied to achieve exceptional refinement in grain structure. This process specially helps brittle and large workpieces. Nie et al. [58, 59] have studied microstructure of AZ91-SiC nanocomposites exposed to MDF. AZ91-SiC nanocomposites possess enhancement in dynamic recrystallization from the very

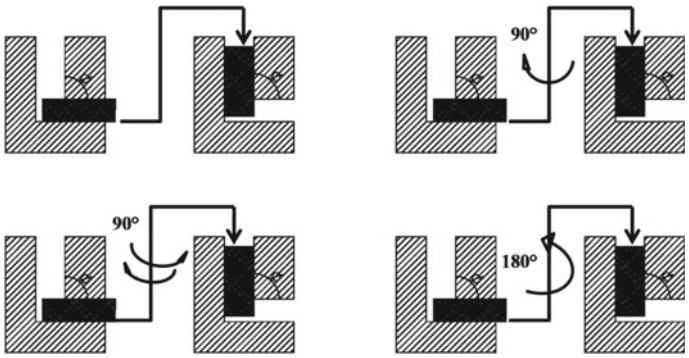

Fig. 8 Schematic diagram of equal channel angular pressing

first pass of MDF. With further increment in passes, conformity of microstructure and recrystallization increased.

3.4 Equal Channel Angular Pressing (ECAP)

ECAP is the process of modifying the microstructure with ultrafine grains (UFG). Schematic diagram of ECAP is shown in Fig. 8. Nanocomposite billet is passed through two identical intersecting channel die (channel intersection angle = Φ). In this process, geometrical cross section of the billet remains same but billet is subjected to extreme plastic deformation (shear), and this step is followed for several passes to generate UFG. Shear strain (γ) of each individual pass is calculated by Eq. 3.

$$\gamma = 2\cot\left(\frac{\Phi}{2}\right) \tag{3}$$

Zhu et al. [77] have suggested that the best result of grain refinement is achieved for $\Phi = 90°$.

3.5 Cyclic Extrusion and Compression (CEC)

CEC is also a severe plastic deformation process in which fine-grained microstructure can be achieved by passing nanocomposite billets in between annual die. Selections of number of passes and temperature are most important for achieving fine grain. Guo et al. [34] have used CEC to achieve fine grain for Mg–SiC nanocomposite. In this study, optimum number of passes and optimum temperature are considered as

up to 8 and 300–400 °C, respectively. Superior grain structure as well as enhanced hardness is obtained.

4 Strengthening Mechanism

Ceramic nanoparticles possess strong effect on yield strength depending on different strengthening mechanisms. Total strength can be determined by calculating the sum of yield strength due to grain refinement (Δ_{GR}), due to Orowan contribution (Δ_{OR}), due to difference in modulus of elasticity (Δ_{MOD}), due to coefficient of thermal expansion (Δ_{CTE}) and due to load-bearing factor (Δ_{LOAD}).

4.1 Orowan Strengthening

In Orowan strengthening, it is considered that particles are almost homogeneously distributed in matrix. These homogeneously distributed nanoparticles obstruct the movement of dislocations through matrix. When they try to interact with particles, the dislocations bend about the particles and connect with other dislocation. As a result, strength increases. Strength maintains inverse relationship with interparticle distance which yields that smaller particles impart higher strength for same volume or mass. Contributions of Orowan strengthening are described by Eq. (4), and interparticle distance (λ) is described by Eq. (5):

$$\Delta\sigma_{OR} = \frac{0.13BG_m}{\lambda} \ln \frac{d_p}{2b} \tag{4}$$

$$\lambda = d_p\left[\left(\frac{1}{2V_p}\right)^{(1/3)} - 1\right] \tag{5}$$

where b = burgers vector, d_p = average dia. of nano-particle, G_m = shear modulus and V_p = volume fraction.

Chen et al. [14] have reported the contribution of Orowan strengthening on yield strength of Mg-1SiC nanocomposite as 113 MPa. It is also yielded that this result is due to small interparticle distance. Cao et al. [10, 11] have performed the Orowan strengthening-related calculations of Mg-1AlN nanocomposite. It is shown that Orowan strengthening has improved yield strength by 44% which is around 35.8 MPa and grain refinement has contributed around 8.2 MPa on yield strength.

4.2 Hall–Petch

Due to the introduction of ceramic reinforcements, primary precipitation occurs at the time of solidification which leads to refinement of grains. Typically, reinforcing nanoparticles in magnesium alloys improve yield strength which results in refinement of grains. Increment of yield strength can be found by Hall–Petch equation (6), in which yield strength (σ_y) is

$$\sigma_y = \sigma_0 + k_y D^{(-1/2)} \tag{6}$$

where σ_0 = friction stress when no strengthening mechanism is present, k_y = stress concentration factor and D = grain size. Again, increment of yield strength for nanocomposites can be calculated by considering same fabrication process for alloy also. In this case, yield strength is found out by following Eq. (7) considering grain size of nanocomposite (D_{MMNC}) and base alloy (D_{O}):

$$\Delta_{\mathrm{GR}} = k_y \left(\frac{1}{\sqrt{D_{\mathrm{MMNC}}}} - \frac{1}{\sqrt{D_{\mathrm{O}}}} \right) \tag{7}$$

Dieringa et al. [21] have added AlN (1 wt%) nanoparticles in AM60 alloy melt and reported that incorporation of AlN nanoparticles has improved yield strength and tensile strength by 103% and 115%, respectively. Again, improvement of yield strength due to grain refinement is calculated as 42.7 MPa and same due to Orowan strengthening is 8.3 MPa.

4.3 Mismatch in the CTE

Usually matrix metal and reinforcement phase have different CTE which results in stresses at interface. Hence, increased difference in CTE generates higher stress which causes geometrical necessary dislocations (GND). GND normally helps to accommodate CTE difference. Typically, GNDs enhance the value of yield strength for nanocomposites like cold working. Yield strength due to CTE ($\Delta\sigma_{\mathrm{CTE}}$) can be computed by following Eq. (8) [71]:

$$\Delta\sigma_{\mathrm{CTE}} = \sqrt{3}\beta G_{\mathrm{m}} b \sqrt{\frac{12 V_{\mathrm{p}} \Delta\alpha \Delta T}{b d_{\mathrm{p}}}} \tag{8}$$

where β = coefficient of dislocation strengthening, $\Delta\alpha$ = CTE difference and ΔT = temperature difference.

4.4 Mismatch in Young's Modulus

Moreover, GNDs can also be created due to mismatch of Young's modulus between matrix and reinforcement phase. To make this happen, nanocomposite must be processed through secondary processing method (extrusion, rolling, etc.). Due to formation of GNDs, yield strength of nanocomposite enhances. Dai et al. [19] have proposed Eq. (9) to compute yield strength ($\Delta\sigma_{\text{Mod}}$) due to distinction of Young's modulus considering ε = bulk strain for composite and α = material coefficient.

$$\Delta\sigma_{\text{Mod}} = \sqrt{3}\alpha G_{\text{m}} b \sqrt{\frac{6V_{\text{p}}\varepsilon}{bd_{\text{p}}}} \tag{9}$$

4.5 Load-Bearing

Load-bearing mechanism is also considered as one strengthening mechanism which contributes in increasing yield strength. Moreover, it is also considered to have small influence as nanocomposites contain small amount of reinforcement. Yield strength due to load-bearing mechanism is calculated by following Eq. (10), where yield strength of base matrix is σ_{m}.

$$\Delta\sigma_{\text{Load}} = \frac{1}{2} V_p \sigma_{\text{m}} \tag{10}$$

5 Mechanical Properties

Basic objective of incorporating nanoparticles in magnesium matrix is to achieve enhanced mechanical properties like hardness, ultimate tensile strength (UTS), yield strength (YS), compressive strength, creep behavior, etc. For this purpose, researchers have incorporated different nanoparticles (Al_2O_3, SiC, Y_2O_3, AlN, TiB_2, WC, CNT) in magnesium base matrix.

5.1 Al_2O_3

Gnanavelbabu et al. [31] have studied the role of ultrasonic power (0, 1500, 2000 and 2500 W) at fixed time and frequency on mechanical properties of AZ91D-1Al_2O_3

nanocomposites. It is reported that microhardness is enhanced 18% for 2500 W UST-treated nanocomposite compared to untreated (0 W UST) nanocomposite. Again, YS, UTS and % elongation of 2500 W UST-treated nanocomposite have improved by 28%, 48% and 10%, respectively. Habibnejad-Korayem et al. [35] have shown that incorporation of nano-Al_2O_3 (2 wt%) in magnesium matrix has significantly improved microhardness and UTS than base alloy. Sameer Kumar et al. [46] have reported that incorporation of n-Al_2O_3 in AZ91E alloy through stir casting method has improved UTS and hardness than AZ91E alloy by 22.5% and 26.54%, respectively. Hassan and Gupta [38] have incorporated 1.1 wt% Al_2O_3 nanoparticle (50 nm) in Mg alloy and studied mechanical properties like microhardness, YS, UTS, elastic modulus and ductility. It was reported that all those mechanical properties have achieved significant enhancement due to presence of Al_2O_3 nanoparticles. Fractography study revealed that Al_2O_3 nanoparticles have activated non-basal slip which changed the fracture behavior from brittle to mixed system.

5.2 SiC

Lan et al. [48] have studied mechanical behavior of Mg-SiC nanocomposites fabricated by UST. It is reported that with incorporation of 5 wt% of n-SiC, microhardness has improved by 75% than base alloy. Nie et al. [61] have used extrusion (at 350 °C) on AZ91D-0.5SiC nanocomposite to enhance mechanical properties. It is concluded that YS and UTS of nanocomposites have increased with increase in extrusion temperature. Shen et al. [66] have synthesized Mg-SiC nanocomposites through semisolid stirring and UST followed by extrusion. Tensile test results indicated that incorporation of 1 vol% SiC has increased UTS and YS to 300 and 225 MPa while incorporation of 2 and 3 vol% of SiC has increased UTS to 335 MPa and 380 MPa, respectively. At same condition (2 and 3 vol% of SiC), YS was increased to 268 and 313 MPa. Bao et al. [8] have successfully incorporated SiC nanoparticles through UST followed by extrusion and achieved UTS as 299 MPa and YS as 220 MPa. Liu et al. [51] have incorporated nano-SiC particles in AZ91D alloy and attained 43.6% and 117% improvement of UTS and YS, respectively.

5.3 AlN

AZ91D was reinforced by AlN nanoparticles (1 wt%), and mechanical properties were studied. It was reported that only 1 wt% of AlN nanoparticle have enhanced YS at room temperature and elevated temperature (200 °C) by 44% and 21%, respectively. Sankaranarayanan et al. [65] have incorporated 0.2 and 0.8 wt% of AlN nanoparticles in pure magnesium. Mg-0.2AlN nanocomposite provided maximum improvement in ductility (85%) while Mg-0.8AlN nanocomposite has provided maximum improvement in tensile strength (30%). In compressive loading condition,

overall strength was improved by 30% without arousing effect on ductility. Katsarou et al. [43] have incorporated AlN nanoparticles in Elektron21 magnesium alloy and studied hardness, mechanical properties and creep resistance. It was reported that incorporation of 1 wt% of AlN has significantly enhanced creep resistance of developed nanocomposite.

5.4 CNT

Goh et al. [33] have developed Mg-1.3CNT nanocomposite and studied fatigue behavior and ductility of developed nanocomposite. It is observed that highly active basal slip has helped to enhance ductility significantly. Liu et al. [52] have incorporated 1.5 wt% CNT and observed improvement in YS, UTS and elongation by 21%, 22% and 42%, respectively, than AZ91D alloy.

5.5 WC

Banerjee et al. [5] have incorporated WC nanoparticles (0, 0.5, 1, 1.5 and 2 wt%) in AZ31 alloy and found that microhardness of Mg-2WC nanocomposite (104.20 $HV_{0.05}$) has enhanced significantly than AZ31 alloy (68.35 $HV_{0.05}$). Similarly, Karuppusamy et al. [42] have fortified 1.5 wt% WC nanoparticle in AZ91 magnesium alloy and compared the mechanical properties between cryogenic-treated (CT) and non-treated nanocomposites. It is reported that Rockwell hardness of CT-nanocomposite has enhanced by 10.5% than non-treated nanocomposite. Again, UTS of cryogenic-treated nanocomposite has improved by 35% than AZ91 alloy. Praveenkumar et al. [63] have developed AZ31-WC composite and studied mechanical properties like microhardness, YS, UTS and flexural strength. It is revealed that all those properties have improved significantly due to the presence of WC and rate of improvement of those properties are increased with increase in wt% of WC.

5.6 TiB_2

Meenashisundaram et al. [54] have incorporated 0.58–1.98 wt% of nano-TiB_2 in magnesium alloy and studied room temperature tensile properties. It is disclosed that Mg-1.98TiB_2 possesses best result and YS, UTS and fracture strain have improved by 54%, 15% and 79%, respectively. Study of compressive properties discloses that Mg-1.98TiB_2 yield strength has improved by 47% while ultimate compressive strength and fracture strain have improved by 10% and 11%, respectively. Choi et al. [17] have reinforced TiB_2 nanoparticles (1 and 2.7%) in AZ91D alloy using UST by applying 20 kHz frequency and generating 60 μm amplitude. Mechanical properties were

Table 1 Observation details [17]

Material	UTS (MPa)	YS (MPa)	E (%)
AZ91	162 ± 3	88 ± 3	2.88 ± 0.12
AZ91 + 1TiB_2	180 ± 1	104 ± 1	3.33 ± 0.05
AZ91 + 2.7TiB_2	188 ± 1	107 ± 1	4.27 ± 0.61

studied at room temperature and found improved strength and ductility. Observation details are tabulated in Table 1.

6 Tribological Properties

6.1 Al_2O_3

Gnanavelbabu et al. [31] have studied tribological properties of AZ91-n-Al_2O_3 composites treated with different UST power (0, 1500, 2000, 2500 W). Wear rate and coefficient of friction (COF) have been evaluated with respect to different sliding speed and load. It has been revealed that tribological properties have enhanced significantly due to enhancement in UST power. At 2500 W, wear rate and coefficient of friction have reduced than other samples in different experimental conditions. It has also been disclosed that adhesion, oxidation, abrasion and delamination are responsible wear mechanism. Lim et al. [50] have incorporated 0.22, 0.66 and 1.11 vol% Al_2O_3 nanoparticle in Mg-matrix and performed tribo-tests by varying sliding velocity at 10 N load. It has been revealed that wear rate has significantly reduced with incorporation of Al_2O_3 nanoparticles. It is also reported that Mg-1.11 Al_2O_3 possesses 1.8 times better wear resistance than base alloy for 10 m/s sliding velocity. Habibnejad-Korayem et al. [35] explored wear characteristics of magnesium, magnesium alloy and Mg-Al_2O_3 by varying sliding velocity and applied load. It is reported that nanocomposite possesses minimum wear rate among developed materials and wear rate follows inverse relation with sliding velocity while wear rate follows direct relation with load. Similarly, Nguyen et al. [57] have discussed wear behavior of AZ31B-Al_2O_3 nanocomposites by comparing load–speed condition. In this study, experiments were carried at 10 N load for different sliding speed (1, 3, 5, 7 and 10 m/s) and at 30 N load for different sliding speed (1, 3 and 5 m/s). It is indicated that wear resistance of nanocomposites has continuously curtailed throughout the speed range and loads. But, wear rate of nanocomposites is surpassing the wear rate of base alloy at low speeds and wear rate of nanocomposites reduced with increased value of sliding speed.

6.2 SiC

Zhang et al. [75] have investigated tribological characteristics of Mg-SiC nanocomposites (10 and 15 wt %) and compared with pure magnesium and AZ31B alloy. This study disclosed that COF of nanocomposites are much higher than AZ31B alloy. COF values of Mg-10SiC are almost similar to AZ31B and nearly 30% greater than commercially pure Mg (C_P-Mg). On the other hand, Mg-SiC nanocomposite displayed lowest wear rate compared to all other materials which is around 23 times lesser to C_P-Mg. Labib et al. [47] have explored wear and friction characteristics of Mg–SiC nanocomposites by varying loads (5–60 N) and temperatures (25–200 °C) at fixed sliding speed (0.4 m/s). At 25 °C, wear rates are almost similar for 5 and 20 N but at higher loads, composites possess far better wear resistance than base alloy. Again, composite maintains lesser wear rate than base alloy at elevated temperatures (100, 150 and 200 °C). Moreover, increase in applied load shifted the characteristics of wear from mild to severe at all temperatures.

6.3 WC

Banerjee et al. [5] have carried out dry sliding wear test of AZ31-WC nanocomposites for varying load and sliding speed systems where load range is 10–40 N and speed range is 0.1–0.4 m/s. It was revealed that wear rate is maximum for base alloy and decreased continuously with increasing percentage of WC. Again, continuous incremental trend of wear rate with respect to sliding speed and applied load was reported for base alloy while nanocomposites offered initial detrimental trend following moderate increment. Moreover, COF yielded continuous detrimental tendency for all experimental conditions. COF of nanocomposites have lower COF than base alloy. COF values for nanocomposites possess incremental trend with increase in weight percentage of WC. Banerjee et al. [6] have again reported the effect of elevated temperature and loads on tribological behavior of Mg-WC MMNCs. Wear rate increased continuously for base alloy but for MMNCs wear rate almost remains unchanged up to a transition limit, after that significant increase was noticed. COF provided slight increment with temperature for both alloy and nanocomposites. Karuppusamy et al. [42] have examined the effect of cryogenic treatment (−190 °C) on wear behavior of AZ91-WC nanocomposite at different experimental conditions. At lower load (20 N), wear rate followed detrimental slope for all samples but at higher load (40 N) wear rate of cryogenic-treated nanocomposite was significantly reduced.

7 Corrosion Behavior

Several researchers have studied corrosion behavior of Mg-MMNCs. But scientific community is splitted into two sides about corrosion characteristics of magnesium composites. Some researchers reported that corrosion resistance is decreased due to presence of reinforcement while others concluded that corrosion resistance is enhanced due to reinforcing agents.

7.1 Al_2O_3

Chan et al. [12] have incorporated alumina particles in AZ91 alloy and performed electrochemical impedance spectroscopy (EIS), potentio-dynamic polarization test and immersion tests in alkaline solution to study corrosion behavior. It was observed that composite possesses more corrosion than base alloy (three times) in 3.5% NaCl solution. Ghasali et al. [30] have incorporated Al_2O_3 and Si_3N_4 nanoparticles in magnesium matrix and reported that nanoparticles possess greater polarization resistance compared to C_p–Mg.

7.2 SiC

Pardo et al. [62] have incorporated SiC particles in magnesium matrix (AZ92) and studied corrosion resistance in neutral salt fog and 3.5 wt% NaCl solution. It was reported that Mg-SiC offered severe corrosion by forming different corrosion by-products in neutral fog solution while higher corrosion resistance is observed for high humidity condition. Zhang et al. [74] have reported corrosion behavior of extruded AZ91-SiC composites by evaluating electrochemical measurement and weight loss calculation. It was disclosed that corrosion resistance has decreased noticeably and accelerated hydrogen reduction with increasing volume percentage of SiC. Similarly, Tiwari et al. [70] have tested corrosion behavior of Mg-SiC composites (6 and 16 vol%) in 1 M NaCl. Composites possess higher corrosion than base alloy and SiC have not contributed that much in controlling corrosion rate.

7.3 Graphene and CNT

Aung et al. [4] have studied the examined corrosion behavior of Mg-CNT in 3.5% NaCl solution and discussed that presence of CNT deteriorates corrosion resistance. Fukuda et al. [28] have also studied galvanic corrosion behavior of Mg-CNT composite and revealed that galvanic corrosion has increased than AZ31 alloy due to

presence of CNT. Endo et al. [22] have incorporated MWCNT in magnesium alloy and examined corrosion behavior in salt water. It was disclosed that corrosion resistivity has significantly enhanced due to MWCNT particles. Funatsu et al. [29] have incorporated CNT in AZ61B magnesium alloy and investigated galvanic corrosion resistance which presented significant enhancement by forming gradient distribution.

7.4 WC

Banerjee et al. [7] have studied corrosion behavior of Mg-WC nanocomposites in 3.5% NaCl solution by varying wt% of WC. Presence of capacitive loop of high and low frequency as well as low-frequency inductive loop was observed in Nyquist plot. Loops signify film generation, mass transfer and pit formation. Tafel plot has provided current density and corrosion potential which revealed Mg-0.5WC provides best corrosion resistance. This study also investigated the role of surface roughness which iterated that surface roughness has direct impact on corrosion behavior. Corrosion resistance increased with decrease in roughness.

7.5 TiC

Jia et al. [41] have developed Mg-TiC composite and examined corrosion behavior in saline environment. It was observed that composites have higher galvanic corrosion and corrosion rate than base alloy. Falcon et al. [27] have developed AZ91E-TiC composites and reported that corrosion resistance and pitting resistance have enhanced due to the presence of TiC particles.

8 Conclusion

Typically, novel Mg-MMNCs are able to provide enhanced tensile property, compressive property, creep resistance, tribological properties and corrosion resistance than base alloy and MMCs. Large number of fabrication methods like primary casting and additional secondary deformations (extrusion, rolling, MDF) are available to develop Mg-MMNCs. In the present study, detail discussions about fabrication methods (primary and secondary), mechanical and tribological properties have been discussed. Indeed, present literatures highlighted that liquid metallurgy (ultrasonic vibration-assisted stir casting method, DMD) methods are more prominent and economical to homogeneously incorporate nanoparticles in magnesium matrix. However, role of some secondary methods is also extensive. That is why detailed discussion on liquid metallurgy-based fabrication methods is discussed here. Mechanisms of cavitation and acoustic streaming for UST are also been discussed in details. Presence of

particles also forms some strengthening mechanism in matrix. Details of those mechanisms are also presented in this study. Role of different nanoparticles like Al_2O_3, SiC, TiB_2, WC, CNT and TiC on mechanical and tribological behavior are discussed here by mentioning related literatures. Mechanical properties like microhardness, UTS, YS and creep behavior are mainly considered and related literatures yielded that presence of nanoparticles normally improves those properties. Literature on tribological behavior disclosed that nanoparticles help to improve wear and friction behavior of Mg-MMNCs at room as well as elevated temperatures. But researchers are split into two groups about corrosion characteristics of magnesium composites. Some researchers reported that corrosion resistance is decreased due to presence of reinforcement while others concluded that corrosion resistance is enhanced due to reinforcing particles. However, most studies are limited to laboratory scale which must be practiced in industrial scale also to reveal the exact potential of Mg-MMNCs. More studies on recyclability, energy efficiency and reliability of Mg-MMNCs are also needed to be performed in recent future.

References

1. Abdullah A, Malaki M, Baghizadeh E (2012) On the impact of ultrasonic cavitation bubbles. Proc. Inst. Mech. Eng Part C J Mech Eng Sci 226:681–694
2. Abdullah A, Pak A, Abdullah MM, Shahidi A, Malaki M (2014) Study of the behavior of ultrasonic piezo-ceramic actuators by simulations. Electron Mater Lett 10:37–42
3. Akbari MK, Mirzaee O, Baharvandi H (2013) Fabrication and study on mechanical properties and fracture behavior of nanometric Al_2O_3 particle-reinforced A356 composites focusing on the parameters of vortex method. Mater. Des. 46:199–205
4. Aung NN, Zhou W, Goh CS, Nai SML, Wei J (2010) Effect of carbon nanotubes on corrosion of Mg–CNT composites. Corros Sci 52(5):1551–1553
5. Banerjee S, Poria S, Sutradhar G, Sahoo P (2019a) Corrosion behavior of AZ31-WC nanocomposites. J Magnesium Alloys 7(4):681–695
6. Banerjee S, Poria S, Sutradhar G, Sahoo P (2019b) Tribological behavior of Mg-WC nanocomposites at elevated temperature. Mater Res Express 6(8):0865c6
7. Banerjee S, Poria S, Sutradhar G, Sahoo P (2019b) Dry sliding Tribological behavior of AZ31-WC nano-composites. J Magnesium Alloys 7:315–327
8. Bao S, Li L, Hong Y, Hu Z (2010) Study on the fabrication of SiCp/AZ31 nanocomposites by high energy ultrasonic vibration and its characteristics. J Plasticity Eng 1:139–143
9. Bhingole PP, Chaudhari GP (2012) Synergy of nano carbon black inoculation and high intensity ultrasonic processing in cast magnesium alloys. Mater Sci Eng A 556:954–961
10. Cao G, Choi H, Oportus J, Konishi H, Li X (2008) Study on tensile properties and microstructure of cast AZ91D/AlN nanocomposites. Mater Sci Eng A 494:127–131
11. Cao G, Kobliska J, Konishi H, Li X (2008) Tensile properties and microstructure of SiC nanoparticle-reinforced Mg-4Zn alloy fabricated by ultrasonic cavitation-based solidification processing. Metall Mater Trans A 39:880–886
12. Chan WM, Cheng FT, Leung LK, Horylev RJ, Yue TM (1998) Corrosion behavior of magnesium alloy AZ91 and its MMC in NaCl solution. Corros Rev 16(1–2):43–52
13. Chen K, Li ZQ, Zhou HZ, Wang WK (2007) Influence of high intensity ultrasonic vibration on microstructure of in-situ synthesized Mg_2Si/Mg composite. T Nonferr Metals Soc 17:s391–s395

14. Chen LY, Xu JQ, Choi H, Pozuelo M, Ma XL, Bhowmick S, Yang JM, Mathaudhu S, Li XC (2015) Processing and properties of magnesium containing a dense uniform dispersion of nanoparticles. Nature 528:539–543
15. Chen LY, Peng JY, Xu JQ et al (2013) Achieving uniform distribution and dispersion of a high percentage of nanoparticles in metal matrix nanocomposites by solidification processing. Scr Mater 69:634–637
16. Choi H, Alba-Baena N, Nimityongskul S et al (2011) Characterization of hot extruded Mg/SiC nanocomposites fabricated by casting. J Mater Sci 46:2991–2997
17. Choi H, Sun Y, Slater BP, Konishi H, Li X (2012) AZ91D/TiB_2 Nanocomposites fabricated by solidification nanoprocessing. Adv Eng Mater 14:291–295
18. Cicco M, Konishi H, Cao G et al (2009) Strong, ductile magnesium-zinc nanocomposites. Metall Mater Trans A 40A:3038–3045
19. Dai L, Ling Z, Bai Y (2001) Size-dependent inelastic behavior of particle-reinforced metal–matrix composites. Compos Sci Technol 61:1057–1063
20. Dieringa H, Huang Y, Wittke P, Klein M, Walther F, Dikovits M, Poletti C (2013) Compression creep response of magnesium alloy DieMag422 containing barium compared with the commercial creep-resistant alloys AE42 and MRI230D. Mater Sci Eng 585:430–438
21. Dieringa H, Katsarou L, Buzolin R, Szakács G, Horstmann M, Wolff M, Mendis C, Vorozhtsov S, StJohn D (2017) Ultrasound assisted casting of an AM60 based metal matrix nanocomposite, its properties, and recyclability. Metals 7:388
22. Endo M, Hayashi T, Itoh I, Kim YA, Shimamoto D, Muramatsu H, Shimizu Y, Morimoto S, Terrones M, Iinou S, Koide S (2008) An anticorrosive magnesium/carbon nanotube composite. Appl Phys Lett 92(6):063105
23. Erman A, Groza J, Li X, Choi H, Cao G (2012) Nanoparticle effects in cast Mg-1 wt% SiCnanocomposites. Mater Sci Eng A 558:39–43
24. Eskin DG, Eskin GI (2014) Ultrasonic treatment of light alloy melts, 2nd edn. CRC Press, Boca Raton, FL, USA
25. Eskin GI (1995) Cavitation mechanism of ultrasonic melt degassing. Ultrason Sonochem 2:S137–S141
26. Eskin GI (1998) Ultrasonic treatment of light alloy metallic melts. Gordon and Breach Science Publishers, Amsterdam, The Netherlands
27. Falcon LA, Bedolla B, Lemus J, Leon C, Rosales I, Gonzalez-Rodriguez JG (2011) Corrosion behavior of Mg–Al/TiC composites in NaCl solution. Int J Corros
28. Fukuda H, Szpunar JA, Kondoh K, Chromik R (2010) The influence of carbon nanotubes on the corrosion behaviour of AZ31B magnesium alloy. Corros Sci 52(12):3917–3923
29. Funatsu K, Fukuda H, Takei R, Umeda J, Kondoh K (2013) Quantitative evaluation of initial galvanic corrosion behavior of CNTs reinforced Mg–Al alloy. Adv Powder Technol 24(5):833–837
30. Ghasali E, Bordbar-Khiabani A, Alizadeh M, Mozafari M, Niazmand M, Kazemzadeh H, Ebadzadeh T (2019) Corrosion behavior and in-vitro bioactivity of porous Mg/Al_2O_3 and Mg/Si_3N_4 metal matrix composites fabricated using microwave sintering process. Mater Chem Phys 225:331–339
31. Gnanavelbabu A, Surendran KS, Kumar S (2020) Influence of ultrasonication power on grain refinement, mechanical properties and wear behaviour of AZ91D/nano-Al_2O_3 composites. Mater Res Express 7(1):016544
32. Goh CS, Wei J, Lee LC, Gupta M (2006) Simultaneous enhancement in strength and ductility by reinforcing magnesium with carbon nanotubes. Mater Sci Eng A 423(1–2):153–156
33. Goh CS, Wei J, Lee LC, Gupta M (2008) Ductility improvement and fatigue studies in Mg-CNT nanocomposites. Compos Sci Technol 68(6):1432–1439
34. Guo W, Wang Q, Ye B, Li X, Liu X, Zhou H (2012) Microstructural refinement and homogenization of Mg–SiC nanocomposites by cyclic extrusion compression. Mater Sci Eng A 556:267–270
35. Habibnejad-Korayem M, Mahmudi R, Poole WJ (2009) Enhanced properties of Mg-based nano-composites reinforced with Al_2O_3 nano-particles. Mater Sci Eng A 519(1–2):198–203

36. Hassan SF, Gupta M (2007a) Development of nano-Y_2O_3 containing magnesium nanocomposites using solidification processing. J Alloys Compd 429:176–183
37. Hassan SF, Gupta M (2007b) Effect of Nano-ZrO_2 particulates reinforcement on microstructureand mechanical behavior of solidification processed elemental Mg. J Compos Mater 41:2533–2543
38. Hassan SF, Gupta M (2005) Enhancing physical and mechanical properties of Mg using nanosized Al_2O_3 particulates as reinforcement. Metall Mater Trans A 36:2253–2258
39. Huang Y, Dieringa H, Kainer KU, Hort N (2014) Understanding effects of microstructural inhomogeneity on creep response—New approaches to improve the creep resistance in magnesium alloys. J Magnes Alloys 2:124–132
40. Ishiwata Y, Komarov S, Takeda Y (2012) Investigation of acoustic streaming in aluminum melts exposed to high-intensity ultrasonic irradiation. In: Proceedings of the 13th international conference on aluminum alloys (ICAA13), Pittsburgh, PA, USA, 3–7 June
41. Jia S, Jia SS, Sun G, Yao J (2005) The corrosion behaviour of Mg alloy AZ91D/TiCp metal matrix composite. In: Materials science forum, vol 488. Trans Tech Publications, pp 705–708
42. Karuppusamy P, Lingadurai K, Sivananth V (2019) Influence of Cryogenic Treatment On As-cast AZ91+ 1.5 wt% WC Mg-MMNC wear performance. In: Advances in materials and metallurgy. Springer, Singapore, pp 185–197
43. Katsarou L, Mounib M, Lefebvre W, Vorozhtsov S, Pavese M, Badini C, Dieringa H (2016) Microstructure, mechanical properties and creep of magnesium alloy Elektron21 reinforced with AlN nanoparticles by ultrasound-assisted stirring. Mater Sci Eng A 659:84–92
44. Khandelwal A, Mani K, Srivastava N, Gupta R, Chaudhari G (2017) Mechanical behavior of AZ31/Al_2O_3 magnesium alloy nanocomposites prepared using ultrasound assisted stir casting. Compos Part B Eng 123:64–73
45. Kubásek J, Vojtech D, Martínek M (2013) Structural characteristics and elevated temperature mechanical properties of AJ62 Mg alloy. Mater Charact 86:270–282
46. Kumar S, Suman KNS, Ravindra K, Poddar P, SB VS (2017) Microstructure, mechanical response and fractography of AZ91E/Al_2O_3 (p) nano composite fabricated by semi solid stir casting method. J Magnes Alloys 5(1):48–55
47. Labib F, Ghasemi HM, Mahmudi R (2016) Dry tribological behavior of Mg/SiCp composites at room and elevated temperatures. Wear 348:69–79
48. Lan J, Yang Y, Li X (2004) Microstructure and microhardness of SiC nanoparticles reinforced magnesium composites fabricated by ultrasonic method. Mater Sci Eng A 386:284–290
49. Li Q, Rottmair CA, Singer RF (2010) CNT reinforced light metal composites produced by melt stirring and by high pressure die casting. Compos Sci Technol 70(16):2242–2247
50. Lim CYH, Leo DK, Ang JJS, Gupta M (2005) Wear of magnesium composites reinforced with nano-sized alumina particulates. Wear 259(1–6):620–625
51. Liu S, Gao F, Zhang Q, Li W (2009) Mechanical properties and microstrutures of nano-sized sic particles reinforced AZ91D nanocomposites fabricated by high intensity ultrasonic assisted casting. Mater Sci Forum 618–619:449–452
52. Liu S-Y, Gao F-P, Zhang Q-Y, Xue Z, Li W-Z (2010) Fabrication of carbon nanotubes reinforced AZ91D composites by ultrasonic processing. Trans Nonferrous Met Soc China 20:1222–1227
53. Malaki M, Xu W, Kasar AK, Menezes PL, Dieringa H, Varma RS, Gupta M (2019) Advanced metal matrix nanocomposites. Metals 9(3):330
54. Meenashisundaram GK, Seetharaman S, Gupta M (2014) Enhancing overall tensile and compressive response of pure Mg using nano-TiB_2 particulates. Mater Charact 94:178–188
55. Murugan S, Nguyen QB, Gupta M (2019) Synthesis of magnesium based nano-composites. In: Magnesium—The wonder element for engineering/biomedical applications. IntechOpen
56. Nguyen QB, Gupta M (2008) Increasing significantly the failure strain and work of fracture of solidification processed AZ31B using nano-Al_2O_3 particulates. J Alloy Compd 459(1–2):244–250
57. Nguyen QB, Sim YHM, Gupta M, Lim CYH (2015) Tribology characteristics of magnesium alloy AZ31B and its composites. Tribol Int 82:464–471

58. Nie KB, Deng KK, Wang XJ, Wang T, Wu K (2017) Influence of SiC nanoparticles addition on the microstructural evolution and mechanical properties of AZ91 alloy during isothermal multidirectional forging. Mater Charact 124:14–24
59. Nie KB, Deng KK, Wang XJ, Wu K (2017) Characterization and strengthening mechanism of SiC nanoparticles reinforced magnesium matrix composite fabricated by ultrasonic vibration assisted squeeze casting. J Mater Res 32:2609–2620
60. Nie KB, Wang XJ, Wu K, Xu L, Zheng MY, Hu XS (2011) Processing, microstructure and mechanical properties of magnesium matrix nanocomposites fabricated by semisolid stirring assisted ultrasonic vibration. J Alloys Compd 509:8664–8669
61. Nie KB, Wang XJ, Xu L, Wu K, Hu XS, Zheng MY (2012) Influence of extrusion temperature and process parameter on microstructures and tensile properties of a particulate reinforced magnesium matrix nanocomposite. Mater Des 36:199–205
62. Pardo A, Merino S, Merino MC, Barroso I, Mohedano M, Arrabal R, Viejo F (2009) Corrosion behaviour of silicon–carbide-particle reinforced AZ92 magnesium alloy. Corros Sci 51(4):841–849
63. Praveenkumar R, Periyasamy P, Mohanavel V, Ravikumar MM (2019) Mechanical and tribological behavior of Mg-matrix composites manufactured by stir casting. Int J Veh Struct Syst (IJVSS) 11(1)
64. Ramirez A, Ma Q, Davis B, Wilks T, St John DH (2008) Potency of high-intensity ultrasonic treatment for grain refinement of magnesium alloys. Scripta Mater 59:19–22
65. Sankaranarayanan S, Habibi MK, Jayalakshmi S, Jia Ai K, Almajid A, Gupta M (2015) Nano-AlN particle reinforced Mg composites: microstructural and mechanical properties. Mater Sci Technol 31(9):1122–1131
66. Shen MJ, Ying WF, Wang XJ, Zhang MF, Wu K (2015) Development of high performance magnesium matrix nanocomposites using nano-SiC particulates as reinforcement. J Mater Eng Perform 24:3798–3807
67. Shiying L, Feipeng G, Qiongyuan Z, Wenzhen L (2009) Mechanical properties and microstructures of nano-sized SiC particle reinforced AZ91D nanocomposites fabricated by high intensity ultrasonic assisted casting. Mater Sci Forum 618–619:449–452
68. Suslick KS, Cline RE, Hammerton DA (1986) The sonochemical hot spot. J Am Chem Soc 108:5641–5642
69. Suslick KS, Matula TJ (1999) Ultrasonic physical mechanisms and chemical effects. In: Webster J (ed) Wiley encyclopedia of electrical and electronics engineering. Wiley, Hoboken, NJ, USA
70. Tiwari S, Balasubramaniam R, Gupta M (2007) Corrosion behavior of SiC reinforced magnesium composites. Corros Sci 49(2):711–725
71. Vogt R, Zhang Z, Li Y, Bonds M, Browning N, Lavernia E, Schoenung J (2009) The absence of thermal expansion mismatch strengthening in nanostructured metal–matrix composites. Scr Mater 61:1052–1055
72. Wang X, Liu W, Xiaoshi Hu, Kun Wu (2018) Microstructural modification and strength enhancement by SiC nanoparticles in AZ31 magnesium alloy during hot rolling. Mater Sci Eng A 715:49–61
73. Zarembo LK (1971) Part III: Acoustic streaming. In: Rozenberg LD (ed) High-intensity ultrasonic fields. Springer, New York, NY, USA
74. Zhang C, Zhang T, Wang Y, Wei F, Shao Y, Meng G, Wu K (2015) Effect of SiC particulates on the corrosion behavior of extruded AZ91/SiCp composites during the early stage of exposure. J Electrochem Soc 162(14):C754–C766
75. Zhang L, Luo X, Liu J, Leng Y, An L (2018) Dry sliding wear behavior of Mg-SiC nanocomposites with high volume fractions of reinforcement. Mater Lett 228:112–115
76. Zhou X, Su D, Wu C, Liu L (2012) Tensile mechanical properties and strengthening mechanism of hybrid carbon nanotube and silicon carbide nanoparticle-reinforced magnesium alloy composites. J Nanomater 1–7
77. Zhu YT, Lowe TC (2000) Observationsand issues on mechanisms of grain refinement during ECAP process. Mater Sci Eng A 291:46–53

78. Zhu SM, Easton MA, Gibson MA, Dargusch MS, Nie JF (2013) Analysis of the creep behaviour of die-cast Mg–3Al–1Si alloy. Mater Sci Eng A 578:377–382
79. Zhu SM, Gibson MA, Easton MA, Nie JF (2010) The relationship between microstructure and creep resistance in die-cast magnesium-rare earth alloys. Scr Mater 63:698–703